

Ultrasonic study of the filled skutterudite compound $\text{Pr}_{1-x}\text{La}_x\text{Fe}_4\text{P}_{12}$ ($x = 0.05$ and 0.15)

**Y Nakanishi¹, T Kumagai¹, M Oikawa¹, T Tanizawa¹,
M Nakamura¹, H Sugawara², Y Aoki³, H Sato³ and M Yoshizawa¹**

¹ Graduate School of Engineering, Iwate University, Morioka 020-8551, Japan

² Faculty of Integrated Arts and Sciences, The University of Tokushima, Tokushima 770-8502, Japan

³ Department of Physics, Tokyo Metropolitan University, Hachioji 192-0397, Japan

E-mail: yoshiki@iwate-u.ac.jp

Received 26 December 2007, in final form 4 April 2008

Published 19 May 2008

Online at stacks.iop.org/JPhysCM/20/255211

Abstract

We have performed ultrasonic measurements on the filled skutterudite compound $\text{Pr}_{1-x}\text{La}_x\text{Fe}_4\text{P}_{12}$ ($x = 0.05$ and 0.15) to investigate the elastic properties and the 4f electric state of Pr ions. La-substitution causes a drastic change of the elastic constants compared with those of $\text{PrFe}_4\text{P}_{12}$, suggesting that the interplay between Pr ions plays a crucial role in the low temperature properties. Characteristic behavior was observed in the temperature dependence of elastic constants C_{11} , $(C_{11} - C_{12})/2$ and C_{44} at low temperatures. The elastic constants exhibit a steep decrease around a ferromagnetic transition. Furthermore, a characteristic dip was observed around 10 K, possibly due to the low-lying 4f levels of the Pr ion formed by a crystalline electric field effect (CEF). The results obtained could be explained reasonably by a pseudo-quartet ground state: $\Gamma_1 - \Gamma_4^{(1)}$. We discuss the CEF ground state of $\text{Pr}_{1-x}\text{La}_x\text{Fe}_4\text{P}_{12}$ and the origin of the ferromagnetic transition induced by the La-substitution.

1. Introduction

Filled skutterudite compounds form an interesting class of materials since they possess a rich variety of physical properties [1–3]. Even in the series of compounds so far considered to be well-localized 4f electronic systems, such as Pr-based, Nd-based and Sm-based ones, one can find physical properties originating from the renormalization of quasi-particles, comprised of hybridized conduction and f electron states [3–6]. Some of them show the Fermi-liquid-like properties of heavy-fermion metals. A unique filled skutterudite crystal structure with space group $Im\bar{3}$, described by the general formula MT_4X_{12} , where M is a rare-earth or an alkaline-earth metal, T is a transition metal of the iron or cobalt group, and X is a pnictide (P, As, or Sb), gives an interesting playground [7]. The possibility of forming quasi-particles with enormously heavy effective masses was first recognized in $\text{PrFe}_4\text{P}_{12}$. This was evidenced in the high electronic specific heat coefficient ($\gamma = 1.4 \text{ J K}^{-2} \text{ mol}^{-1}$) in an applied field, the large T^2 coefficient ($A = 2.5 \mu\Omega \text{ cm}^{-1} \text{ K}^{-2}$) of the electrical

resistivity and the detection of an extremely large mass m^* (of the order of a hundred times the free electron mass m_0) from de Haars–van Alphen effect measurements [3, 5]. Furthermore a clear non-magnetic phase transition occurs at 6.5 K, possibly due to an antiferro-quadrupolar (AFQ) ordering, confirmed by neutron scattering experiments, although a characteristic softening towards the transition temperature is absent from the temperature dependence of the elastic constants in zero magnetic field [8–11]⁴.

Despite substantial efforts devoted to its study during the last decade it is still not clear which physical mechanisms essentially determine the behavior. No consensus has been reached on the key mechanism for the unusual heavy-fermion behavior without a magnetic degree of freedom. One useful strategy is a systematic study from dilution experiments, with either La or Y doping, which explore the single-site and inter-site effects of the Pr ion in $\text{PrFe}_4\text{P}_{12}$. For La doping, the AFQ

⁴ Recently, a model involving a phase transition due to a multipolar moment was proposed in a theoretical study. The AFQ scenario, hence, must now be discarded.

ordering is suppressed rapidly and disappears completely for $x = 0.10$ [12, 13]. Interestingly, a ferromagnetic transition appears at 1.7 K and 2.2 K, respectively, for $x = 0.05$ and $x = 0.15$ in $\text{Pr}_{1-x}\text{La}_x\text{Fe}_4\text{P}_{12}$. The detailed analysis of the nuclear Schottky contribution to the specific heat indicates that the magnitude of the average Pr magnetic moment on each site is estimated to be $0.40 \mu_B/\text{Pr}$ and $0.67 \mu_B/\text{Pr}$, respectively, for $x = 0.10$ and 0.15. Furthermore, the estimated Sommerfeld coefficient γ is $1.4 \text{ J K}^{-2} \text{ mol}^{-1}$ and $1.7 \text{ J K}^{-2} \text{ mol}^{-1}$, respectively, for $x = 0.10$ and 0.15, indicating the presence of the HF state. These experimental facts remind us that a field-induced magnetic moment or/and a magnetic ordering has little to do with the formation of the HF state [12, 13]. Therefore some research groups, including ourselves, claim that the quadrupolar fluctuation of the Pr ions plays a crucial role in forming the unusual HF state. Clarifying this has been the main issue in recent investigations of the Pr-based compounds.

Elastic constant measurements are particularly well suited for study, via the quadrupolar response of the 4f ions and the magnetoelastic interaction. In general the coupling of the acoustic strain ε to the ionic quadrupole moment tensor Q is large and the coefficients of the elastic constants depend in a characteristic manner on the components of the charge susceptibility χ_Γ . As described in detail below, the elastic constants, via the charge susceptibility, measure the diagonal and off-diagonal quadrupolar matrix elements, which correspond, respectively, to the Curie and van Vleck terms in the charge susceptibility. This is analogous to the magnetic susceptibility, which samples the magnetic dipole matrix elements. With the Γ_3 or Γ_5 quadrupolar-active ground state of the Pr (4f²) ions, one can expect typical quadrupolar effects, especially in the temperature dependence of the elastic constants [14–17].

The central aim of our study is to explore the 4f CEF ground state, which is relevant for the quadrupolar moment, and the dilution effect of La ions on the elastic properties. We are also interested in the elastic behavior close to the magnetic transition temperature on dilution. In order to investigate this, ultrasonic measurements were performed on $\text{Pr}_{1-x}\text{La}_x\text{Fe}_4\text{P}_{12}$ for $x = 0.05$ and 0.15 at low temperatures down to 0.5 K which crossed the magnetic transition temperature. Our preliminary report was published in [18].

2. Experimental details

$\text{Pr}_{1-x}\text{La}_x\text{Fe}_4\text{P}_{12}$ ($x = 0.05$ and 0.15) single crystals were grown by a tin-flux method. Each specimen used for the present ultrasonic measurement was cut into a rectangular shape with two axes along $\langle 100 \rangle$ and $\langle 110 \rangle$ directions. The specimens had sizes of $2.02 \times 1.36 \times 1.5 \text{ mm}^3$ and $1.35 \times 1.02 \times 2.5 \text{ mm}^3$, respectively, for $x = 0.05$ and 0.15. By powder x-ray diffraction, we confirmed the cubic-type structure was maintained for $0.05 \leq x \leq 0.15$, with a lattice parameter increasing linearly with increasing x , following Vegard's law.

The sound velocity, as the elastic constant, was measured with an ultrasonic apparatus using a phase comparison method at temperatures down to 0.5 K in magnetic fields up to

12 T. Plates of LiNbO_3 were used for the piezoelectric transducer. The fundamental resonance frequency of the LiNbO_3 transducer is 5–30 MHz. The transducer was glued onto the parallel planes of the sample by the elastic polymer Thiokol. The absolute value of the sound velocity was obtained by measuring the delay time between the ultrasonic echo signals to an accuracy of a few per cent. The elastic constant was calculated as $C = \rho v^2$ by using the sound velocity v and the density ρ of the crystal. The lattice constants of $\text{Pr}_{1-x}\text{La}_x\text{Fe}_4\text{P}_{12}$ at room temperature, $a = 7.81 \text{ \AA}$ and 7.70 \AA , were used for the estimation of the density, $\rho = 5.12 \text{ g cm}^{-3}$ and 5.01 g cm^{-3} , for $x = 0.05$ and 0.15 respectively.

3. Quadrupolar moment–strain interaction

A characteristic elastic softening towards low temperatures, observed in the temperature dependence of the elastic constants is a feature of quantum phenomena. The elastic softening of the localized f electron system can usually be understood as the quadrupolar response of the system to an external strain associated with the sound wave. With Γ_1 symmetry the volume strain $\varepsilon_B = \varepsilon_{xx} + \varepsilon_{yy} + \varepsilon_{zz}$, associated with the bulk modulus $C_B = (C_{11} + 2C_{12})/3$, couples with the Coulomb multipole moment $O_B = O_4^0 + 5O_4^4$. A softening in C_B is a characteristic phenomena of a valence fluctuation system such as SmB_6 . C_B increases with decreasing temperature due to the anharmonicity of the lattice vibration in a compound with stable 4f electrons, and even for Kondo compounds. With Γ_3 symmetry the elastic strains $\varepsilon_v = \varepsilon_{xx} - \varepsilon_{yy}$ and $\varepsilon_u = (2\varepsilon_{zz} - \varepsilon_{xx} - \varepsilon_{yy})/\sqrt{3}$, associated with the transverse $(C_{11} - C_{12})/2$ mode, couple respectively with the quadrupolar moments $O_2^2 = J_{xx} - J_{yy}$ and $O_2^0 = (2J_z^2 - J_x^2 - J_y^2)/\sqrt{3}$. Finally with Γ_5 symmetry, the elastic strain ε_{xy} , associated with the transverse C_{44} mode, couples with the quadrupolar moment O_{xy} . The lowest order term of this perturbation can be described by [13–16]

$$H_{qs} = \sum_i g_\Gamma O_\Gamma(i) \varepsilon_\Gamma. \quad (1)$$

Here, $O_\Gamma(i)$ is the equivalent quadrupolar operator at the i th Pr site and g_Γ (where Γ denotes the irreducible representation of the point group, i.e., Γ_3 and Γ_5) is the coupling constant. The scattering of the conduction electrons by the electric quadrupolar moments of 4f electrons leads to a quadrupolar interaction such as the RKKY mechanism. This means that the quadrupolar moment $O_\Gamma(i)$ of i th Pr site couples with the moments of the other sites via the conduction electrons through the same mechanism as the RKKY interaction. This inter-site quadrupolar interaction can be described by

$$H_{qq} = \sum_i g'_\Gamma \langle O_\Gamma \rangle O_\Gamma(i). \quad (2)$$

Here, g'_Γ is the quadrupolar coupling constant and $\langle O_\Gamma \rangle$ is the mean field of the quadrupolar moment. The temperature dependence of the symmetric elastic constant C_Γ is described by

$$C_\Gamma(T) = C_\Gamma^{(0)}(T) - \frac{Ng_\Gamma^2 \chi_\Gamma^{(s)}(T)}{1 - g'_\Gamma \chi_\Gamma^{(s)}(T)}. \quad (3)$$

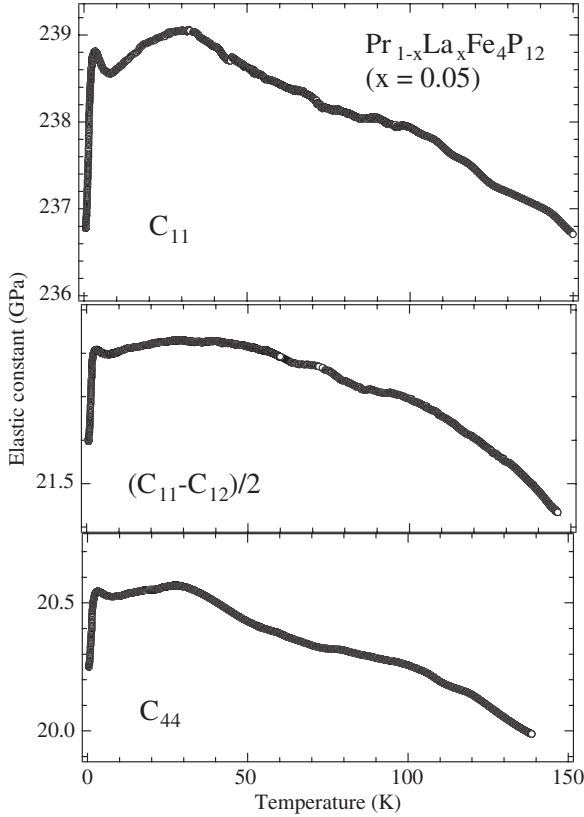


Figure 1. Temperature dependence of elastic constants C_{11} , $(C_{11} - C_{12})/2$ and C_{44} of $\text{Pr}_{0.95}\text{La}_{0.05}\text{Fe}_4\text{P}_{12}$.

Here, N denotes the number of Pr ions in a unit volume, $C_{\Gamma}^{(0)}$ and $\chi_{\Gamma}^{(s)}(T)$ denote respectively the background (without the quadrupolar-strain interaction) and the quadrupolar susceptibility. For the Pr ion in $\text{PrFe}_4\text{P}_{12}$, the Curie term in the quadrupolar susceptibility, due to the Γ_{23} state with orbital degeneracy, gives rise to an elastic softening inversely proportional to temperature at low temperatures in the transverse $(C_{11} - C_{12})/2$ mode, but not in C_{44} . By contrast the Curie term in the quadrupolar susceptibility, due to the $\Gamma_4^{(1)}$ or $\Gamma_4^{(2)}$ states with orbital degeneracy, gives rise to an elastic softening in both $(C_{11} - C_{12})/2$ and C_{44} modes. This distinction generally helps us to determine the 4f ground state of the rare-earth ion in rare-earth compounds.

4. Experimental results

4.1. Elastic properties of $\text{Pr}_{1-x}\text{La}_x\text{Fe}_4\text{P}_{12}$ for $x = 0.05$

Figure 1 shows the temperature dependence of the elastic constants $C_{11}(C_{11} - C_{12})/2$ and C_{44} of $\text{Pr}_{1-x}\text{La}_x\text{Fe}_4\text{P}_{12}$ for $x = 0.05$. The absolute values of each elastic constant and the calculated bulk modulus $C_B = (C_{11} + 2C_{12})/3$ and Poisson's ratio $\gamma_p = C_{12}/(C_{11} + C_{12})$ from C_{11} and $(C_{11} - C_{12})/2$ at both 77 K and 4.2 K of $\text{Pr}_{1-x}\text{La}_x\text{Fe}_4\text{P}_{12}$ for $x = 0.05$ are listed in table 1. The approximate accuracy of the estimated values is better than 5%. C_{11} was measured with longitudinal ultrasonic waves with frequencies of 10 or 30 MHz propagating along the $\langle 100 \rangle$ axis with polarization along the $\langle 100 \rangle$ axis. On the

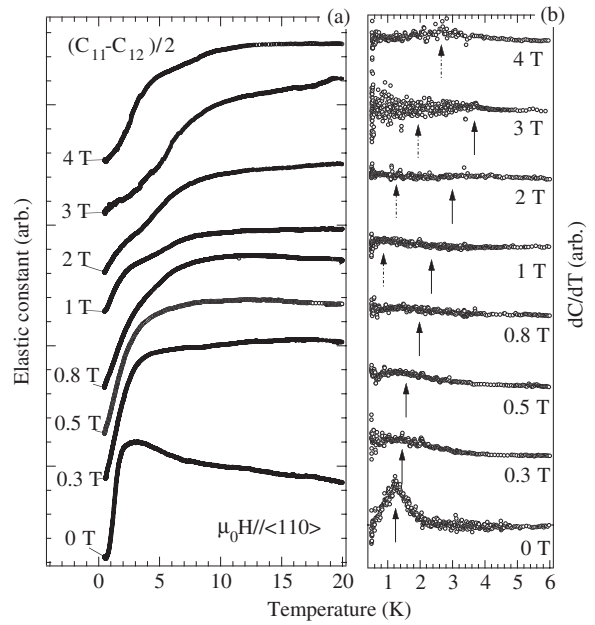


Figure 2. (a) Temperature dependence of the elastic constant $(C_{11} - C_{12})/2$ in selected magnetic fields along the $\langle 110 \rangle$ axis, (b) and that of the derivative of the elastic constant with respect to temperature. Arrows indicate an elastic anomaly recognized in the temperature dependence of the derivative of the elastic constant.

Table 1. The absolute values of the elastic constants, bulk modulus $C_B = (C_{11} + 2C_{12})/3$ and Poisson's ratio $\gamma = C_{12}/(C_{11} + C_{12})$ of $\text{Pr}_{1-x}\text{La}_x\text{Fe}_4\text{P}_{12}$ for $x = 0.05$ and 0.15 at both 77 K and 4.2 K.

Elastic constant	$x = 0.05$ (GPa)		$x = 0.15$ (GPa)	
	77 K	4.2 K	77 K	4.2 K
C_{11}	239	238	264.1	265.5
$(C_{11} - C_{12})/2$	21.8	21.7	35.9	35.8
C_{44}	20.5	20.3	24.1	23.9
$C_B = (C_{11} + 2C_{12})/3$	144.8	144.2	152.1	153.1
$\gamma_p = C_{12}/(C_{11} + C_{12})$	0.449	0.449	0.421	0.422

other hand, $(C_{11} - C_{12})/2$ and C_{44} were measured by transverse ultrasonic waves with frequencies of 5 or 15 MHz propagating along the $\langle 110 \rangle$ axis with polarization along the $\langle 1\bar{1}0 \rangle$ axis, and along the $\langle 100 \rangle$ axis with polarization along the $\langle 010 \rangle$ axis, respectively. The $\text{Pr}_{0.95}\text{La}_{0.05}\text{Fe}_4\text{P}_{12}$ data exhibit near normal behavior at high temperatures: a stiffening with decreasing temperature. However, it is seen that the elastic constants exhibit a marked maximum at 30 K and a lattice softening below that temperature. Surprisingly, a remarkable dip around 10 K, followed by a steep decrease below 2 K appears in the elastic constants. They all stay constant at the lowest temperature of 0.5 K. These prominent features are totally different from those of $\text{PrFe}_4\text{P}_{12}$ reported previously [10].

Figures 2(a) and (b) show the temperature dependence of $(C_{11} - C_{12})/2$ in selected magnetic fields directed along the $\langle 110 \rangle$ axis, combined with the derivative of $(C_{11} - C_{12})/2$ with respect to temperature. The steep drop is gradually suppressed and shifts to higher temperatures with increasing field, which is more clearly seen in the derivative of $(C_{11} - C_{12})/2$ shown in figure 2(b). A hump at around 4 K in a

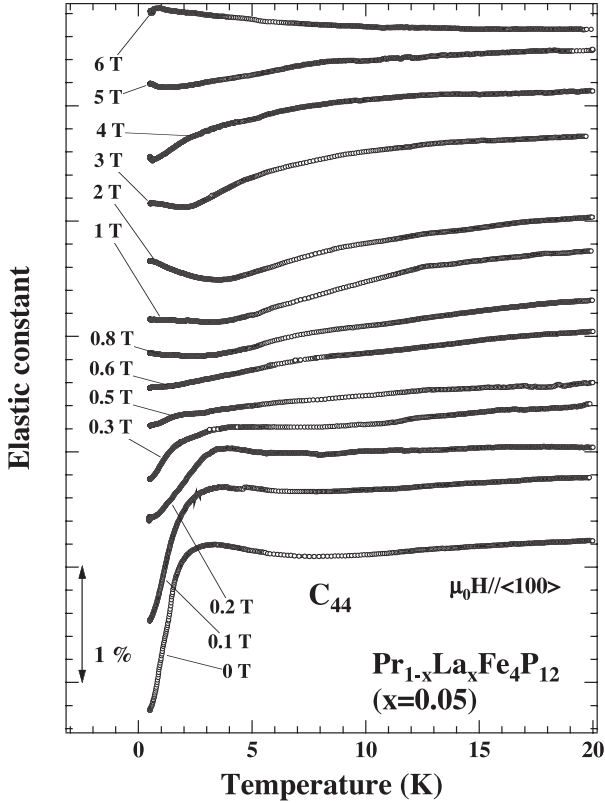


Figure 3. Temperature dependence of the elastic constant C_{44} in selected magnetic fields along the $\langle 100 \rangle$ axis.

magnetic field of 1 T and the field evolution above 1 T are seen. Figure 3 shows the temperature dependence of C_{44} in selected magnetic fields directed along the $\langle 100 \rangle$ axis. C_{44} shows a complicated field dependence at low temperatures. The steep drop of C_{44} below around 2 K is gradually suppressed with increasing magnetic field up to 0.6 T. On a further increase in the field an upturn is observed with a clear dip appearing around 5 K in a magnetic field of 1 T. This dip gradually smears out with increasing magnetic field, and is totally suppressed by the application of a magnetic field of 4 T. Instead, a slight lattice softening shows up in a magnetic field of 4 T. This slight softening is again gradually suppressed on a further increase of the field. In addition, a clear dip observed around 7 K in zero field becomes gradually smaller and shifts to higher temperatures with increasing field. Figure 4 shows the magnetic phase diagram of $\text{Pr}_{1-x}\text{La}_x\text{Fe}_4\text{P}_{12}$ for $x = 0.05$ for fields along the $\langle 100 \rangle$ and $\langle 110 \rangle$ axes as deduced from these results. The circles and squares represent the peaks determined by the temperature dependence of the derivative of the elastic constants with respect to temperature, $dC/dT - T$. The boundary shown by a broken line shifts up with a higher field and gradually vanishes at higher temperatures, reminiscent of the ferromagnetic transition as proposed previously [12, 13].

4.2. Elastic properties of $\text{Pr}_{1-x}\text{La}_x\text{Fe}_4\text{P}_{12}$ for $x = 0.15$

Figure 5 shows the temperature dependence of the elastic constants $C_{11}(C_{11} - C_{12})/2$ and C_{44} of $\text{Pr}_{1-x}\text{La}_x\text{Fe}_4\text{P}_{12}$ for

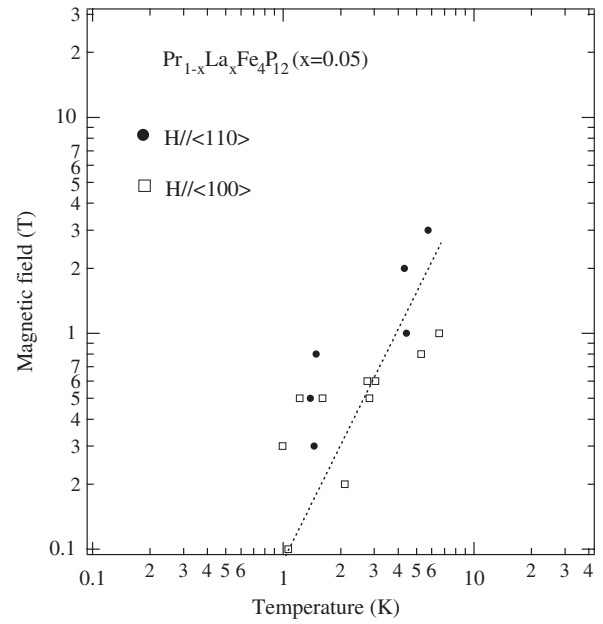


Figure 4. Magnetic phase diagram of $\text{Pr}_{1-x}\text{La}_x\text{Fe}_4\text{P}_{12}$ for $x = 0.05$ deduced from the elastic constants presented in this paper. Solid circles and open squares indicate the elastic anomalies in the selected magnetic fields along the $\langle 100 \rangle$ and $\langle 110 \rangle$ axis, respectively.

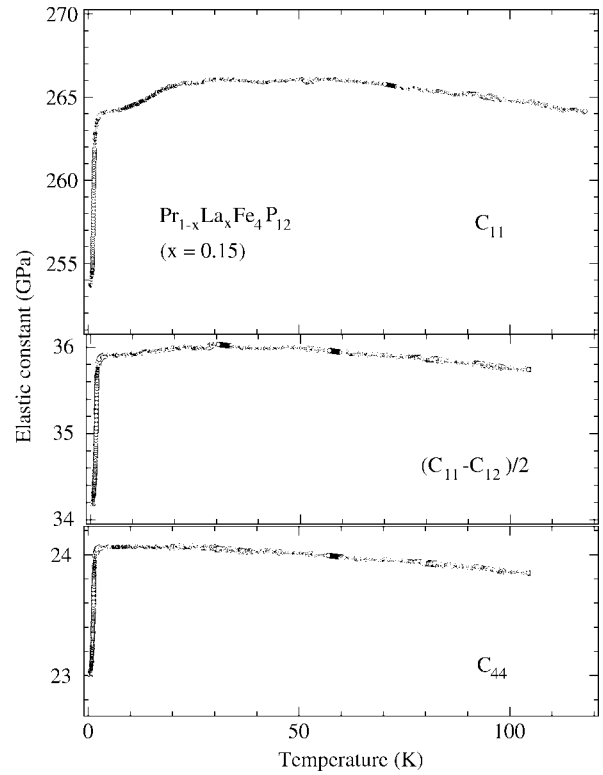


Figure 5. Temperature dependence of the elastic constants C_{11} , $(C_{11} - C_{12})/2$ and C_{44} of $\text{Pr}_{1-x}\text{La}_x\text{Fe}_4\text{P}_{12}$ for $x = 0.15$.

$x = 0.15$. The absolute values of each elastic constant and the calculated bulk modulus $C_B = (C_{11} + 2C_{12})/3$ and Poisson's ratio $\gamma_p = C_{12}/(C_{11} + C_{12})$ from C_{11} and $(C_{11} - C_{12})/2$ at both 77 K and 4.2 K of $\text{Pr}_{1-x}\text{La}_x\text{Fe}_4\text{P}_{12}$

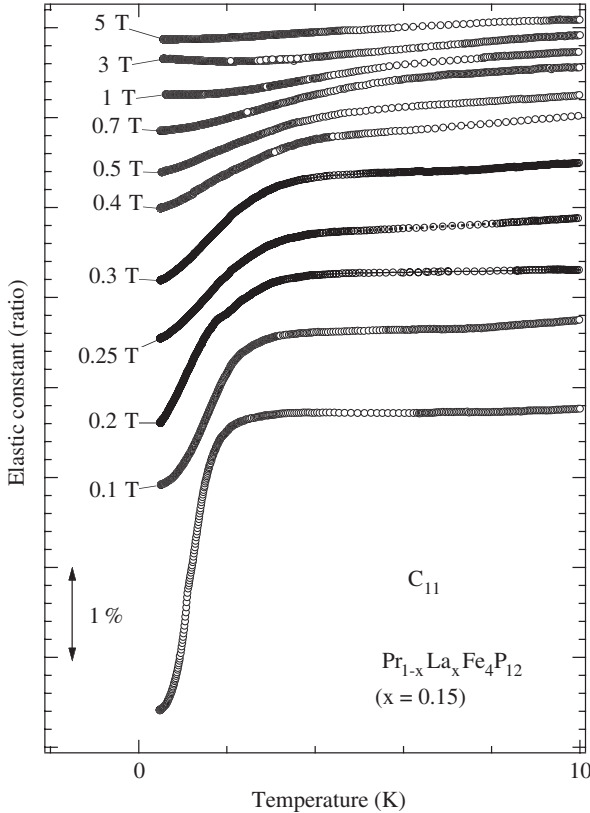


Figure 6. Temperature dependence of the elastic constant C_{11} of $\text{Pr}_{1-x}\text{La}_x\text{Fe}_4\text{P}_{12}$ for $x = 0.15$ in selected fields along the $\langle 100 \rangle$ axis.

for $x = 0.15$ are listed in table 1. The elastic constants exhibit a less complicated field dependence, compared to that for the case of $x = 0.05$. A slight lattice softening starts below about 30 K in C_{11} and $(C_{11} - C_{12})/2$ at zero magnetic field. A steep drop was observed below around 2 K in the elastic constants. They all stay constant at the lowest temperature of 0.5 K. It should be noted that similar behavior: a steep drop, around T_c was also observed in this system with $x = 0.05$. In addition, a slight minimum structure was recognized around 10 K in C_{11} and $(C_{11} - C_{12})/2$. The minimum structure is probably ascribed to the low-energy thermal excitations of the 4f ground state split by the CEF effect, as will be discussed below in detail. Figure 6 shows the temperature dependence of C_{11} in selected magnetic fields directed along the $\langle 100 \rangle$ axis. The steep decrease due to the phase transition becomes gradually smaller with increasing magnetic field, and was suppressed totally by the application of a magnetic field of 5 T. The midpoint of the decrease shifts to higher temperatures, consistent with the specific heat measurement reported previously [12, 13]. Figure 7 shows the field dependence of C_{44} at selected temperatures for a magnetic field along the $\langle 100 \rangle$ axis. A steep increase of C_{44} was observed below the transition temperature of 2.2 K. It is worth noting that C_{44} turns out to be hysteretic, indicating the transition is first order. This magnetic phase transition is, therefore, most likely to be a ferromagnetic one, as proposed previously [12, 13]. In fact, C_{44} shows a decrease without any hysteresis above the

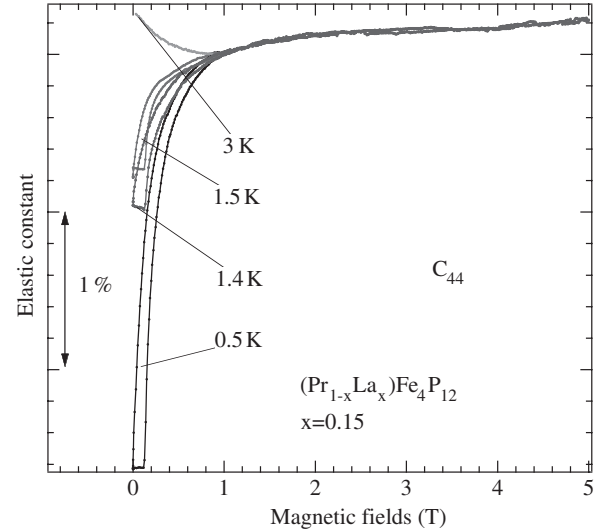


Figure 7. Field dependence of the elastic constant C_{44} of $\text{Pr}_{1-x}\text{La}_x\text{Fe}_4\text{P}_{12}$ for $x = 0.15$ at selected temperatures in a field along the $\langle 100 \rangle$ axis.

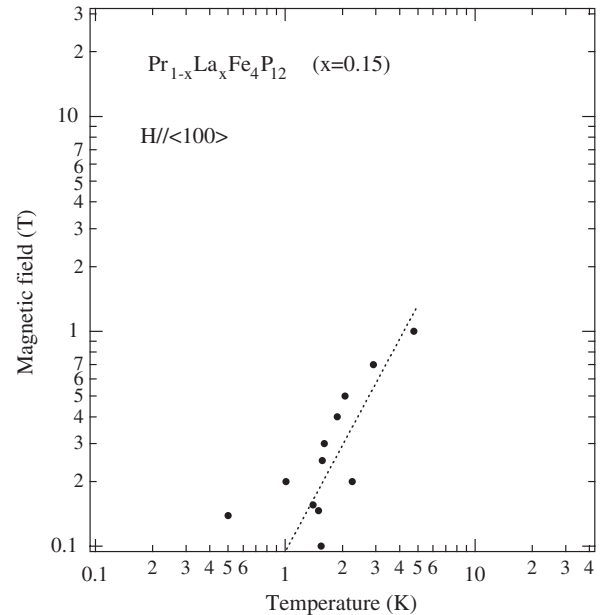


Figure 8. Magnetic phase diagram of $\text{Pr}_{1-x}\text{La}_x\text{Fe}_4\text{P}_{12}$ for $x = 0.15$ deduced from the elastic constants presented in this paper. Solid circles indicate the elastic anomalies in the selected fields along the $\langle 100 \rangle$.

transition temperature. Figure 8 shows the magnetic phase diagram of $\text{Pr}_{1-x}\text{La}_x\text{Fe}_4\text{P}_{12}$ for $x = 0.15$ for a magnetic field along the $\langle 100 \rangle$ as deduced from these results. The solid circles represent the peaks determined by the temperature dependence of the derivative of the elastic constants with respect to temperature $dC/dT - T$. The boundary shown by a broken line shifts up with a higher field and gradually vanishes at higher temperatures, again reminiscent of the ferromagnetic transition, and qualitatively similar to that for $x = 0.05$.

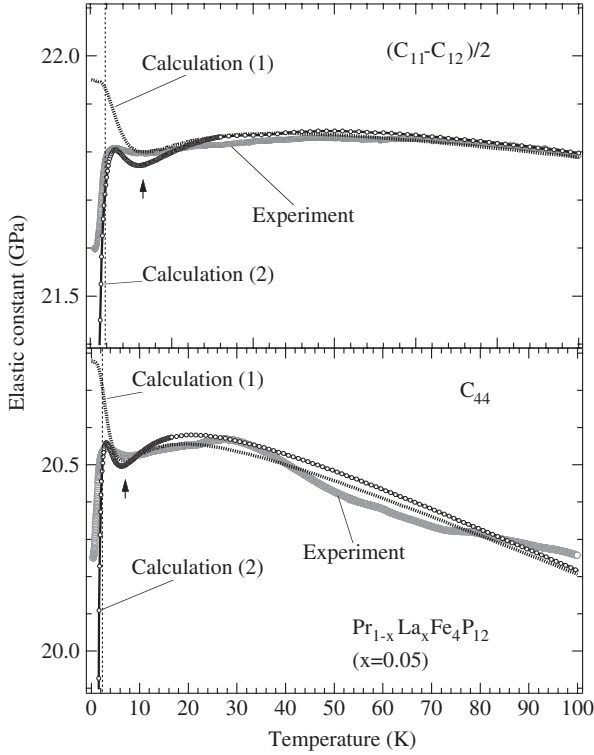


Figure 9. Calculated elastic constants $(C_{11} - C_{12})/2$ and C_{44} for $x = 0.05$ considering the CEF effect, quadrupole-strain and inter-ionic quadrupolar interactions. The pseudo-quartet state $\Gamma_1 - \Gamma_4^{(1)}$ was assumed as single-site CEF levels: Calculation 1 uses (3), and Calculation 2, taking into account the critical behavior, uses (4).

Table 2. The estimated coupling constants g_Γ and g'_Γ for $\text{Pr}_{1-x}\text{La}_x\text{Fe}_4\text{P}_{12}$ for $x = 0.05$ and 0.15 .

	$x = 0.05$		$x = 0.15$	
	$\Delta = 8 \text{ K}$	$\Delta = 10 \text{ K}$	$\Delta = 15 \text{ K}$	
g_{Γ_3} (mK)	1.08	1.37	2.07	
g'_{Γ_3} (mK)	-102	-182	-182	
g_{Γ_5} (mK)	1.43	0.81	1.23	
g'_{Γ_5} (mK)	-98.2	-132	-207	

5. Analyses and discussions

First, we would like to examine the level scheme of a Pr^{3+} ion split into a Γ_1 singlet, a Γ_{23} doublet and two Γ_4 triplets by the cubic crystalline electric field (CEF) effect with T_h symmetry. In the $\text{PrFe}_4\text{P}_{12}$ case the CEF energy splitting has already been studied intensively and some models of the CEF energy scheme have been proposed. However, the crucial energy level scheme has not been explicitly determined to date as the predominant hybridization effect between the conduction bands and the 4f electronic state makes this difficult. On the other hand, we obtained the characteristic behavior of the temperature dependence of the elastic constants in the La-substitution systems presented here, possibly due to the CEF effect.

The degeneracy of the $^2\text{G}_5$ ground state multiplet of Pr^{3+} is partly removed by the influence of the electric charge

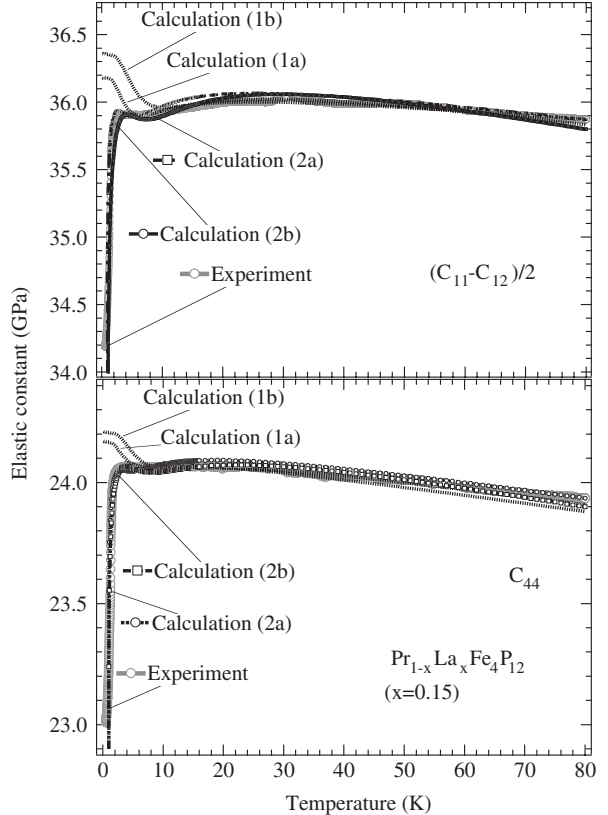
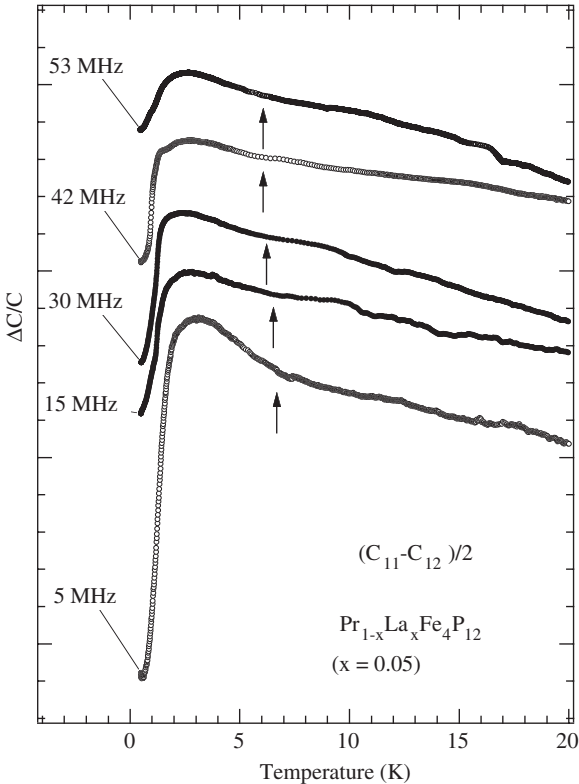


Figure 10. Calculated elastic constants $(C_{11} - C_{12})/2$ and C_{44} for $x = 0.15$ considering CEF effect, quadrupole-strain, inter-ionic quadrupolar interactions. The pseudo-quartet state $\Gamma_1 - \Gamma_4^{(1)}$ was assumed as single-site CEF levels: calculations (1a) and (1b), with the energy difference Δ of 10 K and 15 K respectively, use (3) and calculations (2a) and (2b), with the energy difference Δ of 10 K and 15 K respectively, taking into account the critical behavior, use (4).

distribution of the surrounding ions, i.e. CEF effect. For Pr sites the CEF effect decomposes the Pr^{3+} J-multiplet into a singlet Γ_1 , a doublet Γ_{23} and two triplets $\Gamma_4^{(1)}$ and $\Gamma_4^{(2)}$. Recently, a pseudo-quartet ground state $\Gamma_1 - \Gamma_4^{(1)}$ model has been proposed by theoretical studies [19, 20]. Although it may be disputed, the pseudo-quartet ground state is preferable in reproducing the observed characteristic features. The $\Gamma_1 - \Gamma_4^{(1)}$ model produces a dip in the temperature dependence of $(C_{11} - C_{12})/2$ and C_{44} . The position where the dip appears is strongly dependent on the energy difference Δ between the ground and excited states Γ_1 and $\Gamma_4^{(1)}$. Thus we suppose that the dip structures, observed in the temperature dependence of the elastic constants around 5 K for $x = 0.05$ and 8 K for $x = 0.15$, possibly correspond to the expected minima. The solid and broken lines are fitting curves using the elastic constants described by equation (3) as shown in figures 9 and 10 for $x = 0.05$ and 0.15 respectively. The fitting curves give us an energy difference Δ of 8 K and 10 K or 15 K for $x = 0.05$ and 0.15 , respectively. For these cases we obtain a quadrupole-strain coupling and inter-site quadrupole interaction constants as summarized in table 2. It is noted that, for simplicity, we used only a $\Gamma_1 - \Gamma_4^{(1)}$ partial level scheme with the splitting energy of Δ since the whole explicit CEF level scheme has not been determined, and neither contribute much to the low

Table 3. The estimated physical parameters of $\text{Pr}_{1-x}\text{La}_x\text{Fe}_4\text{P}_{12}$ for $x = 0.05$ and 0.15 .

	$x = 0.05$			$x = 0.15$					
	$\Delta = 8 \text{ K}$			$\Delta = 10 \text{ K}$			$\Delta = 15 \text{ K}$		
β	1.0	0.37	0.50	1.0	0.37	0.50	1.0	0.37	0.50
T_c (K)	0.61	0.61	0.61	0.90	0.90	0.90	0.90	0.90	0.90
$A: (C_{11} - C_{12})/2$	0.31	0.30	0.29	0.50	0.55	0.47	1.1	1.1	1.1
$A: C_{44}$	0.35	0.51	0.44	0.20	0.20	0.22	0.25	0.30	0.34

**Figure 11.** Frequency dependence of $(C_{11} - C_{12})/2$ of $\text{Pr}_{1-x}\text{La}_x\text{Fe}_4\text{P}_{12}$ for $x = 0.05$.

temperature properties. However as readily seen in figures 1 and 5, the steep drop around the magnetic transition remains unexplained in this model.

We attributed the dip observed around 5 K in the temperature dependence of C_{44} to the CEF effect. However, one can speculate that this anomaly might also be attributed to the instability of the rare-earth ions in the highly anharmonic potential formed by a weak coupling of the ions in the Fe_4P_{12} polyanion cage, so called ‘rattling’, since the behavior is somehow similar to that observed in other systems with the $\text{Os}_4\text{Sb}_{12}$ polyanion cage [21–23]. However, there have been no reports concerning rattling in Fe_4P_{12} polyanion cases to date. In fact, as can be seen in figure 11 the anomaly does not show any frequency dependence. Hence, this possibility is presumably ruled out.

Finally, we would like to discuss the steep decrease that is possibly due to the magnetic transition. $\text{Pr}_{1-x}\text{La}_x\text{Fe}_4\text{P}_{12}$ exhibits a steep drop, followed by a smooth bending at the magnetic transition temperature, in contrast to a clear

cusp behavior as often observed in well-localized 4f electron systems. The isostructural system of $\text{NdFe}_4\text{P}_{12}$ is the typical example, showing a ferromagnetic ordering at $T_c = 1.9 \text{ K}$ [24]. It should be noted that one can find similar behavior at the magnetic transition in some other skutterudite compounds such as $\text{CeOs}_4\text{Sb}_{12}$, $\text{SmFe}_4\text{P}_{12}$ and $\text{SmOs}_4\text{Sb}_{12}$ as previously reported [25–27]. Interestingly, they all exhibit a ferromagnetic ordering at low temperatures, accompanied by a release of an extremely small entropy below the transition temperature at which the heavily renormalized quasi-particle bands are considered to be formed. The existence of a ferromagnetic interaction among rare-earth ions is immediately deduced. Hence, they seem to have the same origin although this interpretation is not yet clearly understood.

We now discuss the critical behavior of the elastic constants around T_c in $\text{Pr}_{1-x}\text{La}_x\text{Fe}_4\text{P}_{12}$. When a treatment of the elastic constants around T_c is made based on the usual Ginzburg–Gaussian approximation, we can attempt to fit the data presented here by [28–30]

$$C_\Gamma(T) = C_\Gamma^{(0)}(T) - A(T - T_c)^{-\beta}, \quad (4)$$

where $C_\Gamma^{(0)}$ is the background elastic constant and β is a critical exponent for an order parameter: $\beta = 0.5$ (3D Gaussian), 0.37 (3D X–Y model) and 1 (2D Gaussian). The fits can reasonably reproduce the experimental results. We were, however, able to obtain the most acceptable fits with $\beta = 0.5$ as shown in figures 9 and 10.

The obtained parameters of the fits are summarized in table 3. We cannot yet conclude which is the crucial order parameter to bring about the phase transition. The clear decrease in the elastic constants, accompanied by a small induced magnetic moment reminds us of a multipolar ordering, such as a octupolar ordering, proposed in phase II of $\text{SmRu}_4\text{P}_{12}$ and in phase IV of $\text{Ce}_{1-x}\text{La}_x\text{B}_6$ with $x \sim 0.75$. The pseudo-quartet ground state $\Gamma_1 - \Gamma_4^{(1)}$ could provide a suitable base, for example, for an octupole ordering [31–34].

We now believe that the data presented here of $\text{Pr}_{1-x}\text{La}_x\text{Fe}_4\text{P}_{12}$ for $x = 0.05$ and 0.15 could be explained reasonably by the quadrupolar susceptibility and critical behavior due to the ferromagnetic transition, described by the formula (3) and (4), respectively.

6. Concluding remarks

In this paper we have presented the elastic properties of $\text{Pr}_{1-x}\text{La}_x\text{Fe}_4\text{P}_{12}$ for $x = 0.05$ and 0.15 . We have measured the temperature and the field dependence of the elastic constants C_{11} , $(C_{11} - C_{12})/2$ and C_{44} . A characteristic softening towards

low temperature probably suggests a ground state with orbital degeneracy. The proposed low-lying level scheme, the $\Gamma_1-\Gamma_4^{(1)}$ quartet, can reasonably reproduce the dip structure observed in the temperature dependence of the elastic constants. A clear anomaly, relating to a phase transition, was observed at T_c , accompanied by a clear hysteresis behavior, which is indicative of a first-order transition. Although the crucial order parameter is still unknown, an itinerant ferromagnetic order derived from mobile electrons is one of the most plausible candidates to explain this. The microscopic details of the magnetic structure in the ordered state will only be fully understood after detailed experiments such as neutron scattering, nuclear magnetic resonance and resonant x-ray scattering measurements. Furthermore, it will be necessary to perform the same measurements on $\text{Pr}_{1-x}\text{La}_x\text{Fe}_4\text{P}_{12}$ with other concentrations and we are planning to do this in the near future.

Acknowledgments

The measurements were performed in the Cryogenic Division of the Center for Instrumental Analysis, Iwate University. This work was supported by a Grant-in-Aid for Science Research Priority Area ‘Skutterudite’ (No. 15072202) of the Minister of Education, Culture, Sports, Science, and Technology of Japan.

References

- [1] Szytula A and Leciejewicz J 2003 *Handbook on the Physics and Chemistry of Rare Earths* vol 33, ed K A Gschneider Jr, J-C G Bunzli and V K Pecharsky (Amsterdam: Elsevier) p 1
- [2] Torikachvili S M, Chen W J, Dalichaouch Y, Guertin P R, McElfresh W M, Rossel C and Maple B M 1987 *Phys. Rev. B* **36** 8660
- [3] Sato H, Abe Y, Okada H, Matsuda D T, Abe K, Sugawara H and Aoki Y 2000 *Phys. Rev. B* **62** 15125
- [4] Sugawara H, Abe Y, Aoki Y, Sato H, Hedo M, Settai R, Onuki Y and Harima H 2000 *J. Phys. Soc. Japan* **69** 2938
- [5] Sugawara H, Matsuda T D, Abe K, Aoki Y, Sato H, Nojiri S, Inada Y, Settai R and Onuki Y 2002 *Phys. Rev. B* **66** 134411
- [6] Takeda N and Ishikawa M 2001 *J. Phys.: Condens. Matter* **13** 5971
- [7] Takegahara K, Harima H and Yanase A 2001 *J. Phys. Soc. Japan* **70** 1190
- [8] Hao L, Iwasa K, Nakajima M, Kawana D, Kuwahara K, Kohgi M, Sugawara H, Matsuda T D, Aoki Y and Sato H 2003 *Acta Phys. Pol. B* **34** 1113
- [9] Iwasa K, Hao L, Kohgi M, Sugawara H, Aoki Y and Sato H 2003 *Acta Phys. Pol. B* **34** 1117
- [10] Nakanishi Y, Shimizu T, Yoshizawa M, Matsuda T D, Sugawara H and Sato H 2001 *Phys. Rev. B* **63** 184429
- [11] Kiss A and Kuramoto Y 2006 *J. Phys. Soc. Japan* **75** 103704
- [12] Namiki T, Aoki Y, Yamada Y, Matsuda T D, Sugawara H and Sato H 2002 *Physica B* **312/313** 825
- [13] Aoki Y, Namiki T, Matsuda T D, Sugawara H and Sato H 2002 *J. Phys. Chem. Solids* **63** 1201
- [14] Lüthi B 1985 *J. Phys. Chem. Solids* **52** 70
- [15] Mullen M E, Lüthi B, Wang P S, Bucher E, Longinotti L D, Maita J P and Ott H R 1974 *Phys. Rev. B* **10** 186
- [16] Nakamura S, Goto T, Ishikawa Y, Sakatsume S and Kasuya M 1994 *J. Phys. Soc. Japan* **63** 623
- [17] Thalmeier P 1988 *J. Magn. Magn. Mater.* **76/77** 299
- [18] Nakanishi Y, Oikawa M, Tanizawa T, Kumagai T, Yoshizawa M, Saha S R, Sugawara H, Kaneyama T, Aoki Y and Sato H 2006 *Physica B* **378–380** 220
- [19] Kiss A and Kuramoto Y 2005 *J. Phys. Soc. Japan* **74** 2530
- [20] Hotta T 2005 *J. Phys. Soc. Japan* **74** 1275
- [21] Goto T, Nemoto Y, Sakai K, Yamaguchi T, Akatsu M, Yanagisawa T, Hazama H, Onuki K, Sugawara H and Sato H 2004 *Phys. Rev. B* **69** 180511(R)
- [22] Nemoto Y, Yamaguchi T, Horino T, Akatsu M, Yanagisawa T, Goto T, Suzuki O, Dönni A and Komatsubara T 2003 *Phys. Rev. B* **68** 184109
- [23] Nakanishi Y, Oikawa M, Kumagai T, Sugawara H, Sato H and Yoshizawa M 2005 *Physica B* **359–361** 910
- [24] Nakanishi Y, Kumagai T, Yoshizawa M, Sugawara H and Sato H 2004 *Phys. Rev. B* **69** 064409
- [25] Nakanishi Y, Kumagai T, Oikawa M, Tanizawa T, Yoshizawa M, Sugawara H and Sato H 2007 *Phys. Rev. B* **75** 134411
- [26] Nakanishi Y, Tanizawa T, Fujino T, Sugawara H, Kikuchi D, Sato H and Yoshizawa M 2006 *J. Phys. Soc. Japan* **75** 192
- [27] Nakanishi Y, Tanizawa T, Fujino T, Sun P, Nakamura M, Sugawara H, Kikuchi D, Sato H and Yoshizawa M 2006 *J. Phys.: Condens. Matter* **51** 251
- [28] Yoshizawa M, Goto T and Fujimura T 1982 *Phys. Rev.* **26** 1499
- [29] Suzuki T, Yoshizawa M, Goto T, Yamakami T, Takahashi M and Fujimura T 1983 *J. Phys. Soc. Japan* **52** 1669
- [30] Migliori A, Visscher William M, Wong S, Brown S E, Tanaka I, Kojima H and Allen P B 1990 *Phys. Rev. Lett.* **64** 2458
- [31] Yoshizawa M, Nakanishi Y, Kumagai T, Oikawa M, Sekine C and Shirotan I 2004 *J. Phys. Soc. Japan* **72** 315
- [32] Yoshizawa M, Nakanishi Y, Oikawa M, Sekine C, Shirotan I, Saha S R, Sugawara H and Sato H 2005 *J. Phys. Soc. Japan* **74** 2141
- [33] Suzuki O, Goto T, Nakamura S, Matsumura T and Kunii S 1998 *J. Phys. Soc. Japan* **67** 4243
- [34] Suzuki O, Nakamura S, Akatsu M, Nemoto Y, Goto T and Kunii S 2005 *J. Phys. Soc. Japan* **74** 735